ACS Sustainable Chemistry & Engineering

pubs.acs.org/journal/ascecg

Research Article

Unsorted Postconsumer Plastic Waste in Energy Conversion Using Piezoelectric, Triboelectric, and Pyroelectric Generation Mechanisms

Petr Slobodian, Pavel Riha, and Berenika Hausnerova*

Cite This: ACS Sustainable Chem. Eng. 2025, 13, 2683−2693

Read Online

ACCESS | Metrics & More | Article Recommendations | Supporting Information

ABSTRACT: This study investigates the energy-harvesting potential of unsorted postconsumer plastic packaging waste through piezoelectric, triboelectric, and pyroelectric regimes. The waste included typical commodity polymers such as high-density polyethylene (HDPE), polypropylene (PP), polystyrene (PS), and polyethylene terephthalate (PET). When employed as contact layers of nanogenerators, heterogeneous waste plastic blends demonstrated the ability to convert mechanical and thermal inputs into electrical energy, facilitated by physical contacts among plastics and mechanical deformation of processing additives in plastics as well as temperature gradients. Significant results include output voltage values above 130 V, short-circuit current density, and charge density of 50 ± 2 μAcm^{-2} and 390 ± 21 nCm^{-2}, respectively, obtained for the triboelectric pair of PET bottle film and the blend of PS/HDPE/PP enriched with 60 wt % of PET. Furthermore, the so-called rejected recyclable plastic waste, which is a residual fraction of plastic waste still largely landfilled, generated output voltages above 60 V when paired with a PET bottle in triboelectric device. These findings reveal that unsorted plastic waste has a promising capacity for energy harvesting, indicating its potential for use in sustainable energy applications.

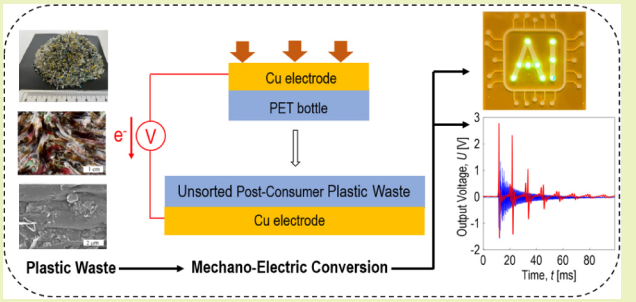

KEYWORDS: *postconsumer plastic waste, rejected recyclable plastic waste, electricity harvesting, nanogenerator*

INTRODUCTION

The current focus on reusing, recycling, and refurbishing products, machinery, and infrastructure increases the opportunity to bring new functionalities into the waste. This is particularly relevant for plastic materials, which since the 1950s have increasingly replaced traditional materials such as glass, wood, and even metals. In 2023, the global plastics market was valued at 712 billion U.S. dollars.[1] Currently, reusing postproduction waste is being successfully managed by most production companies; however, issues related to the recycling of postconsumer plastic waste still persist. Although mechanical recycling is the most straightforward strategy,[2] the complexity of sorting arising from polymer diversity and economic inefficiency results in a substantial portion of postconsumer waste being landfilled or forwarded to chemical recycling using pyrolysis, gasification, hydrocracking, IH2 (integrated hydropyrolysis 2), and KDV (Katalytische Drucklose Verolung) techniques, as well as biomimetic approaches.[3] Furthermore, there remains a fraction called rejected recyclable plastic waste (RRPW), which does not fulfill the minimum quality requirements; therefore, its potential for recycling[4] is negligible, regardless of the effort spent to incorporate RRPW particles, for example, into construction materials.[5]

A key theme of this study is that unsorted plastic packaging waste from postconsumer sources can be converted into electric energy using piezoelectric, triboelectric, and pyroelectric regimes without any demanding techniques or treatment.

Concerning piezo-, tribo-, and pyro-electrification of polymers, polyvinylidene fluoride (PVDF) and its copolymers with trifluoroethylene (PVDF-TrFE), hexafluoropropene (PVDF-HFP), and chlorotrifluoroethylene (PVDF-CTFE) have been the most widely explored (most recently in refs. [6−11]). Fluoropolymers are also often employed to increase the triboelectrification of plastic waste materials. Han et al.[12] prepared a triboelectric nanogenerator (TENG) based on waste plastic bags and polytetrafluoroethylene (PTFE), with an output voltage of 251 V and a short circuit current 34.1 μA. Rani et al.[13] used discarded cigarette filters made of cellulose acetate and recycled aluminum foil as a positive triboelectric material and a plastic waste mixture identified as polyethylene terephthalate (PET), polypropylene (PP), polyvinyl chloride (PVC), and PTFE as a negative triboelectric material and achieved 42.8 V voltage and 0.86 μA current under a

Received: August 22, 2024
Revised: January 30, 2025
Accepted: February 4, 2025
Published: February 12, 2025

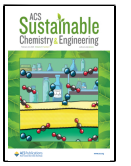

https://doi.org/10.1021/acssuschemeng.4c06984
ACS Sustainable Chem. Eng. 2025, 13, 2683−2693

Table 1. Summary of the Performance and Applications of Contact-Separation Mode Nanogenerators Using Different Triboelectric Waste Plastics

Triboelectric pair	Electrodes	Contact area (cm)	Output voltage (V)	Output current (mA)	Power density (W/m^2)	Application
PS/PS (laminates)[16]	Al/Al	2.5 × 2.5	200	12	0.077	Vibrational energy harvester
Paper/PET bottle[17]	Conductive paste	4.5 × 7	83.8	-	0.260	Energy harvester
PA/PVC[18]	Gold/Gold	3 × 4	35.7	5.8	0.150	Energy harvester
Al/PVC[19]	Cu/Al	3.5 × 3.5	35	-	0.022	Energy harvester
Silicone/saline bottle[20]	Al/Al	5 × 5	508	-	8.780	Sleep monitoring
PET (Mylar)/PP[21]	Cu/Cu	2 × 3	200	-	0.071	Powering electronic gadgets
Glass/laboratory waste (PET)[22]	Al/Al	2.5 × 2.5	185	1.25	0.800	Human tracking device
PU foam/PP[23]	Al/Al	3 × 3	16	-	0.003	Dynamic force sensor

compression force of 10 N with a frequency of 0.1 Hz. Waste expanded polystyrene (PS) was employed to prepare microporous films through solution casting and combined with PTFE as the opposite triboelectric layer by Nawaz et al.[14]

Our goal is to provide an alternative electromechanically responsive high value-added material without environmental issues connected to fluoropolymers and restrictions on the manufacturing, supply, and use of most per- and polyfluorinated alkyl substance materials such as PVDF or PTFE, under the EU's chemicals regulation (REACH), which is expected to come into force in 2025. In 2024, Sherrell et al.[15] reviewed nonfluoro-based piezoelectric and triboelectric polymers, ferroelectric elastomers, and flexoelectric polymers as alternatives for mechanical-to-electrical energy harvesting.

Table 1 summarizes the performance and applications of contact-separation mode nanogenerators using various triboelectric waste plastics. Their advantages lie in a) resource efficiency, offering a cost-effective and environmentally friendly alternative to virgin commodity polymers, PVDF, and other tribological and piezoelectric materials; b) multimodal energy harvesting: energy harvesting is possible from triboelectric, piezoelectric, and pyroelectric effects; c) easy and fast fabrication, using simple pressing and/or extrusion instead of high-tech treatment (e.g., solving, electrospinning, incorporation of nanoparticles); and d) potential for broad applications, resulting from efficient and low-cost raw materials (especially for self-powered sensors, where small energy is acceptable). On the other hand, there are some possible drawbacks of plastic materials in general, which must be considered prior to application to nanogenerators: a) material inconsistency arising from compositional variations, which might be severe for plastic waste mixtures; b) limited lifespan and durability: waste plastics may degrade faster under constant mechanical stress or high temperatures than virgin materials; and c) consistency and standardization: ensuring consistent energy output from mixed-waste plastics remains a primary challenge.

In this work, waste of packaging plastics fabricated from polyethylene terephthalate (PET), polystyrene (PS), high-density polyethylene (HDPE), and polypropylene (PP) is directly ("direct-cut sample"), without any demanding preparation/fabrication techniques, subjected to mechanical electrification in order to find out possible synergistic effects of compounds prepared from the individual wastes in compositions reflecting their typical content in postconsumer waste containers on the obtained output voltages. Nanogenerators using unsorted waste compounds and postconsumer waste fractions rejected from the recycling process have not been reported heretofore. Furthermore, a rather unexplored pyroelectricity of plastic waste is presented. Together with simple application examples of self-powered sensors, this study suggests a new functionality for postconsumer plastic waste.

EXPERIMENTAL SECTION

Materials and Characterization Methods. The tested food packaging plastic compounds were prepared from soft drink bottles, meat packaging trays, cheese packaging trays, and dishwashing liquid bottles. Infrared spectroscopy (FTIR, Nicolet iS5 FTIR Spectrometer, Thermo Fisher Scientific, Waltham, MA, USA) using the ATR technique with a germanium crystal, and Omnic software was employed to confirm the identification of the plastics according to the plastic classification provided by the Society of the Plastics Industry. The CO_2 background spectra were subtracted, and each spectrum represented an average of 64 scans.

The melting temperatures and enthalpies of the wastes were determined with differential scanning calorimetry (DSC 1, PerkinElmer, Waltham, MA, USA). The sample for the DSC analysis weighed approximately 7 mg and was cut from a sample of blended plastic waste. First, the DSC sample was melted at a temperature of about 20 °C above the highest melting point (250 °C) to erase the previous thermomechanical history. Then, the molten blend was cooled down to 20 °C at a rate of 10 °C/min and kept for a minute isotherm prior to increasing the temperature at a heating ramp of 10 °C/min until 280 °C. The DSC melting temperatures were obtained as the maximum melting peak temperatures, and the melting enthalpies as the peak areas below the extrapolated baseline.

Relative permittivity was measured using a broadband dielectric/impedance analyzer (Novocontrol Technologies GmbH & Co. KG, Montabaur, Germany). Samples of a particular thickness were placed between two gold-plated electrodes with a diameter of 20 mm and tested in the frequency range from 1 Hz to 1 MHz at room temperature. A 3D scanner (Zygo NewView 8000, AMETEK, Inc., Middlefield, Connecticut, USA) was used for surface scanning of the tested films and copper (Cu) electrodes. An interferometric system with coherence scanning interferometry (CSI) technology combines the vertical scanning interferometry (VSI) and the phase shifting interferometry (PSI). Surface roughness parameters were measured according to the ISO 21920−2 standard. Mechanical properties were measured with a tensile test machine (M350−5CT, Tensometric, Manchester, UK) at a velocity of 10 mm/min.

https://doi.org/10.1021/acssuschemeng.4c06984
ACS Sustainable Chem. Eng. 2025, 13, 2683−2693

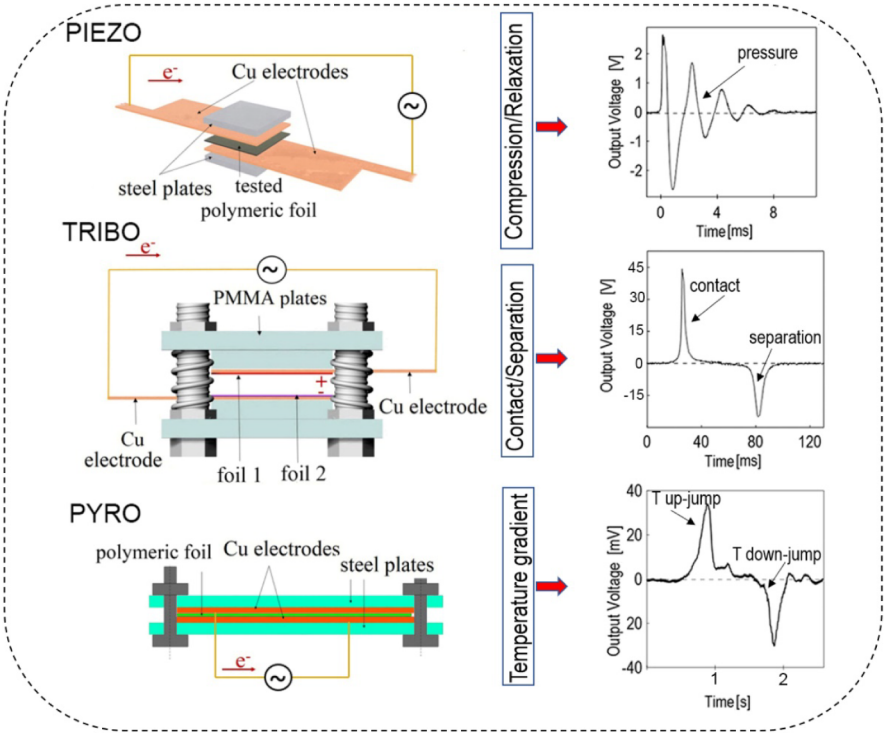

Figure 1. Schematic of sensing electric response to pendulum impact (PIEZO regime), triboelectric nanogenerator (TRIBO regime), and electricity generation by an imposed temperature gradient (PYRO-regime).

Experimental Setup. Electricity generation was carried out using the experimental setup schematically illustrated in Figure 1, where packaging waste plastics were subjected to pressure (piezoelectric regime), contact-induced electrification (triboelectric regime), and a temperature gradient (pyroelectric regime). The test specimen (25 × 25 mm) was sandwiched between the electrodes of a glass−epoxy composite (thickness of 0.25 mm) with a layer of Cu foil (thickness of 35 μm), as shown in Figure 1 PIEZO. The anode was connected to the upper electrode, which was then impacted by a pendulum.

Two steel plates (25 × 25 mm, 5 mm thick) were placed above and below the sample to ensure a uniform distribution of mechanical pulses and provide mechanical protection. The entire assembly was prepressed with an elastic adhesive tape, exerting a pressure force of approximately 2 kPa on the polymer films. A mechanical stimulus was applied by a pendulum that struck the upper protective steel plate. A pendulum (Polymer Test, Versta, Zlin, Czech Republic) with an impact energy of 0.5 J and a velocity of 2.1 m/s was equipped with a strain gauge L6D-C3−40 kg (Zemic Europe B.V., Etten-Leur, The Netherlands) to measure the applied force of the pendulum; the maximum pressure applied by the impact was 148 kPa. An analog converter TZA11410 (VTS Zlin s.r.o., Zlin, Czech Republic) was used to power it with a ± 20 mA output and a 24 V DC supply. An oscilloscope (Infinivision 1000 x-series, 4ch, 100 MHz, DSOX1204A, Keysight, Santa Rosa, CA, USA) was used to measure the generated voltage; the electrodes were covered with metal plates against damage. The charge generated in one cycle was measured using a Vernier CRG-BTA charge sensor (Vernier, Beaverton, OR, USA) connected to the LabQuest interface system (Edufor s.r.o., Prague, Czech Republic). The short-circuit current was calculated from Ohm's law when one cycle of the triboelectric nanogenerators was discharged through an electric resistive load of 27 kΩ, measured by an oscilloscope connected in parallel with the load.

Figure 1 TRIBO regime shows a schematic of a dominantly triboelectric nanogenerator with a vertical contact separation mode, which was implemented in ref. 24 The PMMA plates with copper electrodes were equipped with four metal guides and springs to allow their movement upon touching. A waste sample was attached to the first electrode, and another waste sample was attached to the second electrode as a triboelectric pair material. The electrodes were made from a double-faced adhesive Cu tape with a thickness of 35 μm; the area of the electrodes was (25 × 25) mm. The tested polymeric films were fixed onto the electrodes by sticking to the adhesive layer of the electrically conductive Cu tape (no other dielectric material was added to this experimental setup). The triboelectric pairs were cyclically pressed from a distance of 6 mm against each other at a velocity of approximately 0.75 m/s and a maximum pressure between the contacting polymers of 270 kPa.

A system to perform cyclic mechanical loading using a push-type electromagnet (solenoid) for stability tests was developed to ensure high reproducibility and allow for the precise evaluation of changes in both the electrical output and structural properties of the tested materials. The experiment was conducted in triboelectric contact-separation mode. A circular steel cylinder with a Cu electrode holding the tested sample was fixed to the movable piston of the solenoid. The electrodes had a diameter of 25 mm. The counterpart copper electrode, holding the other material from the tribological pair, was positioned on a stationary granite table. The initial distance between the samples was set to 20 mm, and the solenoid provided cyclic mechanical loading at a frequency of 1

https://doi.org/10.1021/acssuschemeng.4c06984
ACS Sustainable Chem. Eng. 2025, 13, 2683−2693

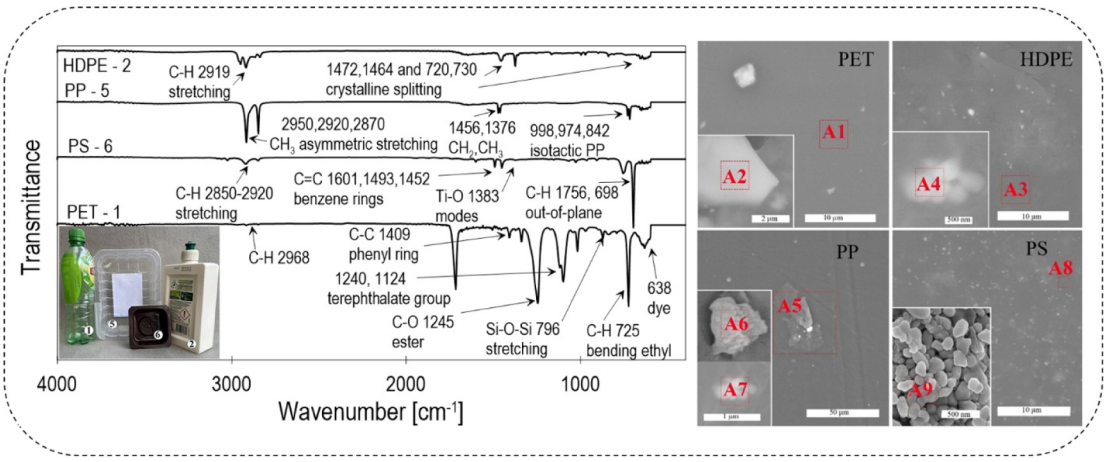

Figure 2. FTIR (Nicolet iS 5 FTIR Spectrometer, Thermo Fisher Scientific) spectra and SEM/EDX (NOVA NanoSEM 450, FEI Co.) analysis of surfaces of used plastic packaging waste and cross sections of their blends and close-up view of added fillers in the inserted images.

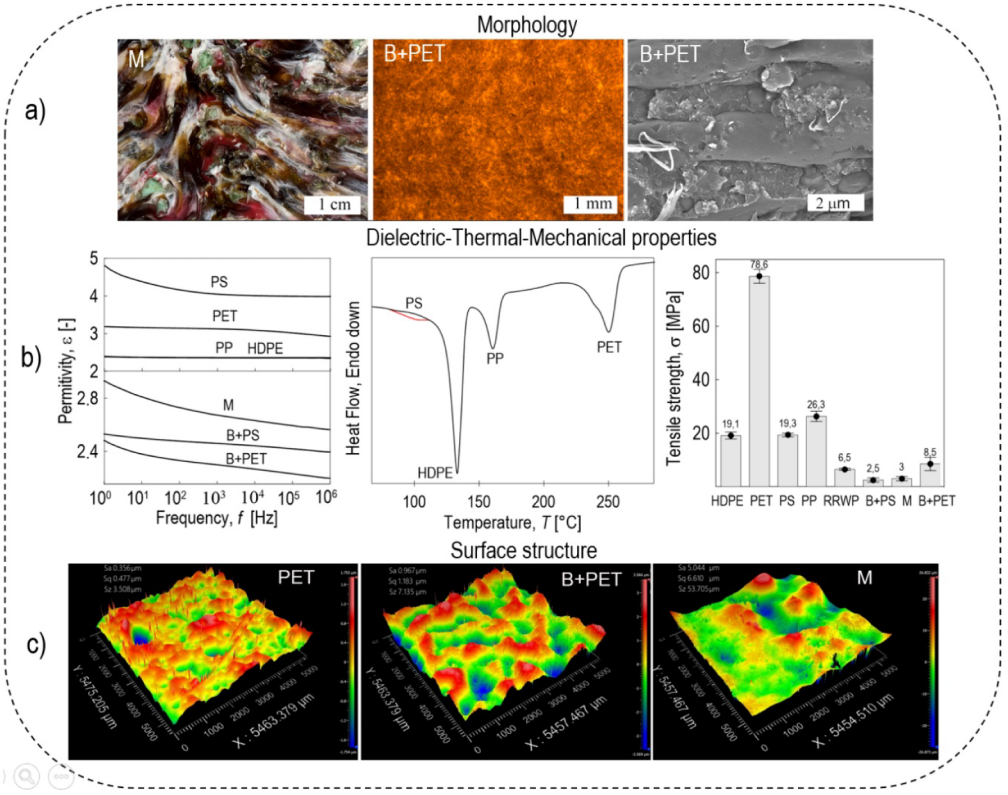

Figure 3. Relevant physical properties of tested plastic waste: a) morphology of compression molded mixture M, melt-mixed blend B+PET, and its detail (SEM, NOVA NanoSEM 450, FEI Co.), b) relative permittivity (Novocontrol Technologies GmbH & Co. KG), transition temperatures (DSC 1, PerkinElmer), tensile strength (M350−5CT, Tensometric), and c) examples of 3D surface scans (Zygo NewView 8000, AMETEK, Inc.) to determine surface roughness parameters (Sa: arithmetical mean height, Sq: root-mean-square height, and Sz: maximum height).

Hz, with a velocity of 0.63 m/s and a maximum impact pressure of 14 kPa.

Temporal temperature gradients were applied to generate pyroelectricity in the tested samples (Figure 1 PYRO). The tested polymer film was equipped with copper electrodes on two sides and fixed between two steel heat-exchange plates (60 × 30 mm) with four screws. Temperature drops were obtained by transferring the polymer films between the thermostatic baths maintained at constant temperatures.

RESULTS

Infrared spectroscopy of packaging wastes revealed polyethylene terephthalate (PET), polystyrene (PS), high-density polyethylene (HDPE), and polypropylene (PP) (Figure 2). A PET bottle was produced by thermoforming an injection-molded sandwich, and other packagings were obtained by thermoforming the melt-extruded films. All packaging plastics contained processing aids, mostly SiO_2 or TiO_2, which are added by packaging manufacturers to enhance their processability.[25] Their distribution in the plastic waste was analyzed using scanning electron microscopy (SEM, NOVA NanoSEM

https://doi.org/10.1021/acssuschemeng.4c06984
ACS Sustainable Chem. Eng. 2025, 13, 2683−2693

Table 2. Surface Roughness Parameters and Thicknesses of the Tested Films

Parameter	HDPE	PP	PS	PET	M	B+PET	B+PS
Sa (μm)	2.315	0.879	0.989	0.356	5.044	4.668	4.567
Sq (μm)	2.948	1.107	1.252	0.477	6.610	4.231	5.845
Sz (μm)	19.744	7.286	8.053	3.508	53.705	7.135	8.625
Thickness (mm)	0.67	0.43	0.34	0.22	0.13	0.13	0.13
STD (mm)	0.027	0.014	0.018	0.014	0.01	0.01	0.01

450, FEI Co., Hillsboro, OR, USA) at an accelerating voltage of 10 kV (Figure 2). Specimens for the analysis of the distribution of inorganic filler particles at the cross sections were obtained by breaking the plastics after cooling in liquid nitrogen. Energy-dispersive X-ray spectroscopy (EDX) revealed the composition of the solid particles observed both on the surface and at the cross-section of the waste.

The filler particles in the PET bottle film were observed as light spots, and their diameters were in the range of 0.2−20 μm. The EDX analysis of area *A1* shows the presence of carbon and oxygen corresponding to the pure PET matrix, whereas area *A2* contains silicon as evidence of the addition of SiO_2 to reduce friction during film production. The shapes of the SiO_2 particles (*A2*) reflect their production via milling. The particles create protrusions on the surface of the film, leading to the reduction of unwanted electric charges that affect the processing. SEM analysis of the HDPE dishwashing liquid bottle (*A3*) confirmed scattered clusters of filler particles with sizes between 0.5 and 3 μm built of individual particles (300−600 nm) of an oval shape. The EDX analysis (*A4*) confirmed the presence of titanium dioxide (TiO_2), which was added as a pigment and to improve the mechanical properties. Furthermore, Si (0.2 wt %), denoting SiO_2 presence in the HDPE matrix, was detected too.

The PP matrix also contained solid particles of different compositions from individual particles of size 0.2−1 μm to various aggregates in the size of tens of micrometers. EDX analysis of the particle marked *A5* showed a wide spectrum of not only 97.9 wt % of C and 3.3 wt % of O but also 0.2 wt % of Na, 0.6 wt % of K, 0.2 wt % of Si, 0.7 wt % of Cl, and 2.1 wt % of Ti. Analysis of the two most common types of aggregates revealed that *A6* area consisted of ferric pigment (65.4 wt % of C, 15.4 wt % of C, 12.6 wt % of Fe, and traces of Na, K, F, Si, Co). The particle depicted in the *A7* area corresponds to the $CaCO_3$ filler (6.7 wt % of Ca). Elements such as Cl, Na, K, and traces of S were attributed to surfactant residues. The PS packaging film was mainly filled with TiO_2. A detailed picture shows the individual TiO_2 particles of an oval shape and sizes from 1.8 to 2.2 μm after dissolving the coating in methyl ethyl ketone and centrifugation.

A mixture (referred to as mixture M in the following text) containing PET/PS/HDPE/PP in a ratio of 25:25:25:25 wt % was prepared by crushing the waste into 4 mm chips in a Retsch Rotor Beater Mill (SR 200, Retsch—Milling and Sieving, Haan, Germany) and processed by compression molding at 200 °C, where PET is below its melting temperature, and thus PET particles are evenly distributed in the matrix formed by other polymers. Second, blends were prepared from HDPE, PP, PS, and PET in a molten state (MB 50 mixer Brabender GmbH & Co. KG, Duisburg, Germany) at 265 °C for 10 min at 50 rpm, and the testing samples were compression-molded at a lower temperature (190 °C) to preserve the structure of an immiscible polymer blend with relatively small, well-separated domains originating from the individual wastes. The B+PET blend contained 60 wt % of PET and the rest 40 wt % evenly divided among PS, HDPE, and PP, and the blend B+PS was composed of 60 wt % of PS and 40 wt % evenly divided among PET, HDPE, and PP.

Microscopic observations (Leica Microsystems Vertrieb GmbH, Wetzlar, Germany; NOVA NanoSEM 450, FEI Co., Hillsboro, OR, USA) revealed a structure composed of rigid domains resulting from the phase separation of these polymers (Figure 3a).

Immiscibility was further confirmed by calorimetry (Figure 3b). As an amorphous polymer, polystyrene has a glass transition temperature response that is not as distinct as the melting temperatures of semicrystalline PET, PP, and HDPE. To make the glass transition temperature (T_g) peak of PS more distinct, the polymer was subjected to physical aging for 10 h below the PS glass transition temperature (90 °C), and then, it was heated to T_g of approximately 98 °C.

The relative permittivity at low frequencies of mixture M (2.9) and blends B+PS (2.5) and B+PET (2.4) fit among those of the individual wastes (PS (4.8), PET (3.2), PP (2.4), and HDPE (2.3)). Tensile tests (Figure 3b and Supporting Information) showed an expected decrease in the strength of the waste mixture and the blends in comparison to individual waste plastics. The poor mechanical properties of mixed plastic waste are a significant obstacle to its reuse in traditional applications, where strength and durability are critical requirements.[26] However, this limitation is not a barrier to sensor applications. Sensors typically require lightweight materials that serve as functional components rather than structural components; thus, mechanical strength is not a primary consideration.

The surface roughness (Figure 3c) parameters and the thickness of the films prepared from the individual wastes, as well as their mixture and blends, are summarized in Table 2 (note that the thicknesses of the individual waste films are those of the packaging products employed in the study). The arithmetical mean of the surface roughness (Sa), the root-mean-square roughness (Sq), and the maximum height of the surface (Sz) confirmed the coarsest surface of the mixture prepared by simple compression molding of the evenly distributed ground (not melted) individual wastes. The roughness parameters of the Cu electrode revealed a very fine surface with Sa = 0.621 μm, Sq = 0.731 μm, and Sz = 4.369 μm.

The electrification of the mixed plastic waste was first tested in response to the mechanical compressive stress generated by a pendulum. During one pendulum impact, the tested sample was compressed to induce an initial voltage. The subsequent fading elastic vibrations of the film (after pendulum rebound) resulted in voltage vibrations, which disappeared within a few milliseconds (Figures 4 and 5).

Because the initial voltage peak is positive, it indicates that electrons are conducted away from the upper electrode via the anode. Considering the dielectric polarization, the negative

https://doi.org/10.1021/acssuschemeng.4c06984
ACS Sustainable Chem. Eng. 2025, 13, 2683−2693

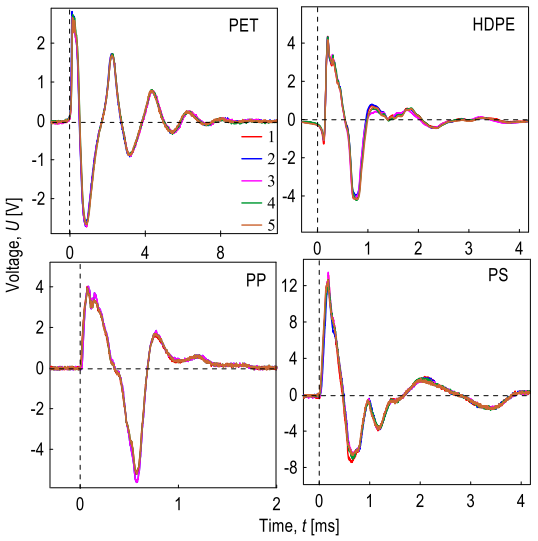

Figure 4. Responses of the individual plastic postconsumer packaging waste to pressure pulses after pendulum impact; five identical cycles.

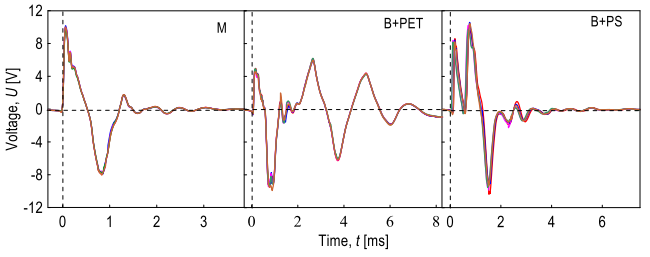

Figure 5. Responses of plastic waste mixture M, blend B+PET, and blend B+PS to pressure pulses after pendulum impact; five identical cycles.

side of the dipoles is oriented upward toward the region where deformation begins owing to the impact, where the deformation is the highest over time, or where a deformation gradient occurs. The obtained voltage outputs increase for various waste combinations: mixture M containing PET/PS/HDPE/PP in a ratio of 25:25:25:25 wt % as well as blend B+PET containing 60 wt % of PET and the rest 40 wt % evenly divided among PS, HDPE and PP, and blend B+PS having 60 wt % of PS and the rest evenly divided among PET, HDPE, and PP.

The nanogenerator built according to Figure 1 TRIBO dominantly measures the triboelectric response of waste plastics (Figure 6). When polymers or polymer blends are paired with PET in a triboelectric pair, except for HDPE, all of them act as tribo-positive relative to PET. However, when PET is paired with HDPE, PET becomes tribo-positive during the electrification.

The measured peak output voltages of the nanogenerators increased from approximately 5 V (short-circuit current density of 2 μAcm^{-2} and power density of 4 μWcm^{-2}) for HDPE/PET to approximately 45 V (short-circuit current density of 18 μAcm^{-2} and power density of 338 μWcm^{-2}) for PP/PET, and to more than 50 V (short-circuit current density of 20 μAcm^{-2} and power density of 417 μWcm^{-2}) for PS/PET. The lowest values of the peak output voltage (4 V), and corresponding 2 μAcm^{-2} and 3 μWcm^{-2}, were obtained for mixture M with evenly represented waste plastics PET, PS, HDPE, and PP in the triboelectric pair with the PET bottle.

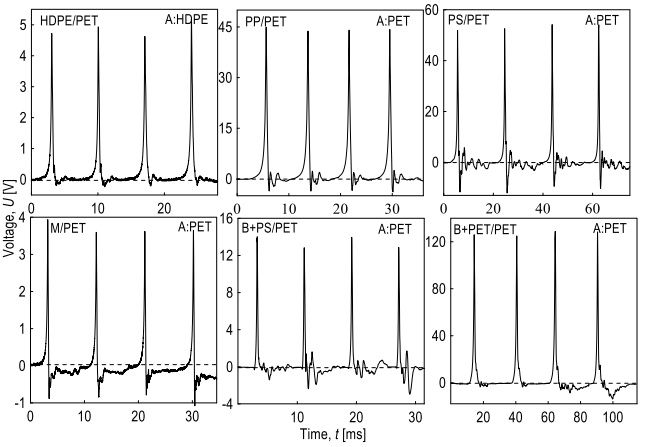

Figure 6. Output voltage as a function of time of the triboelectric nanogenerators made from triboelectric pairs of HDPE, PP and PS packaging plastics waste with PET bottles, their mixture M, blend B+PET, and blend B+PS.

Slightly higher output voltage values (15 V, 6 μAcm^{-2} and 38 μWcm^{-2}) were measured for the PS-enriched blend B+PS paired with PET, and the highest values (peak output voltage in one cycle of 130 V, short-circuit current density of 50 μAcm^{-2} and power density of 2604 μWcm^{-2}) were obtained for the B+PET/PET pair.

The pyroelectric effects (Figure 7) of the packaging plastics and their blends were examined by using the experimental

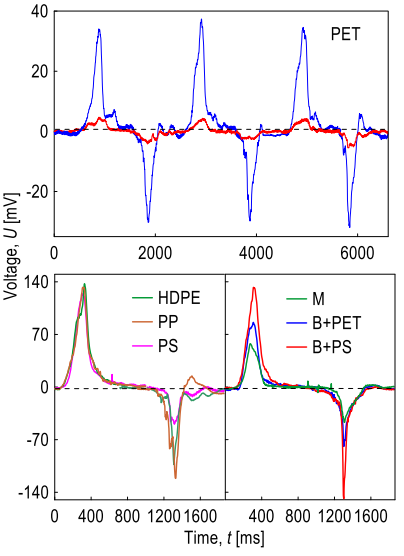

Figure 7. Pyroelectric effect of the individual plastic packaging wastes: mixture M, blend B+PET, and blend B+PS.

setup shown in Figure 1 (PYRO). The results for the PET bottle film are shown for a cyclic temperature change from −10 to 110 °C and back to −10 °C (blue line), and from 10 to 80 °C and back to 10 °C (red line). In the first case, the heating/cooling gradient was approximately 5 °C/s, in the second case 1.5 °C/s. Figure 7 also shows the output pyroelectric voltage values when individual waste packaging plastics and their mixtures were gradually inserted into the temperature changed from −10 to 110 °C and back to −10 °C with the heating/cooling gradient of approximately 5 °C/s.

https://doi.org/10.1021/acssuschemeng.4c06984
ACS Sustainable Chem. Eng. 2025, 13, 2683−2693

Waste packaging plastics are sensitive to both positive and negative changes in the temperature. The generated pyroelectric voltages, on the order of tens of microvolts, were significantly lower than the voltages obtained from the piezoelectric and triboelectric regimes. However, the output voltages of approximately 140 mV obtained with HDPE, PP, and PS are within a similar range as that of a hybrid pyro-piezoelectric TiC-$Ti_3C_2O_2$ nanogenerator prepared from PET bottles, titanium oxide, and lithium carbonate, and endorsed with perovskite-based gel electrolytes.[27]

To demonstrate the harvesting potential of the unsorted plastic waste, the generated AC voltage of the tribological pair PET/B+PET was converted to a DC voltage by using a full-bridge rectifier, as shown in Figure 8. The rectifier was

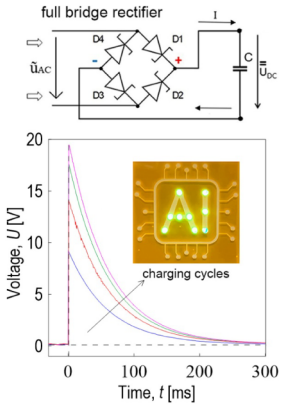

Figure 8. Schematic of full-bridge rectifier based on Schottky diodes with a storage capacitor, time dependency of the discharge of triboelectric pair PET/B+PET for various electrification cycles, and lighting of 9 LED diodes.

equipped with four Schottky diodes (diode-opening voltage of 1.5 V) and the charge was stored in a mica capacitor (capacitance of 4 nF). After charging the capacitor, the circuit was short-circuited after 20 charging cycles. The duration of the lighting for the nine LED diodes was approximately 8 ms.

The time dependence of the discharge for various numbers of electrification cycles is shown in Figure 8. The harvested charge was short-circuited after 5, 10, 15, and 20 charging cycles, and the time-dependent discharge voltage was measured using an oscilloscope. After the short circuit, the voltage response reaches a significant maximum and then decays exponentially to zero over time. The discharge times ranged up to 250 ms after the short circuit, and they were independent of the initial charge level of the capacitor, that is, the number of cycles. The size of the peak increased with increasing storage cycles.

The practical use of energy induced from packaging plastic waste according to the arrangement shown in Figure 1 PIEZO is demonstrated by a sensor that detects the vibrations of sieve analysis equipment. The sensor was placed on the equipment (Figure 9). The surface of the sensor was loaded with a weight by creating a pressure of ∼4 kPa, and the thickness of the plastic waste was ∼0.25 mm.

The energy from waste packaging plastics induced largely by the triboelectric effect was used as a sensor to detect the vibrations of a cantilever beam (Figure 9 TRIBO). The cantilever was 160, 30, and 3 mm long, wide, and thick, respectively. A 0.3 mm thick film of waste plastics (B+PET blend) was pressed in a molten state (at 190 °C) onto the free

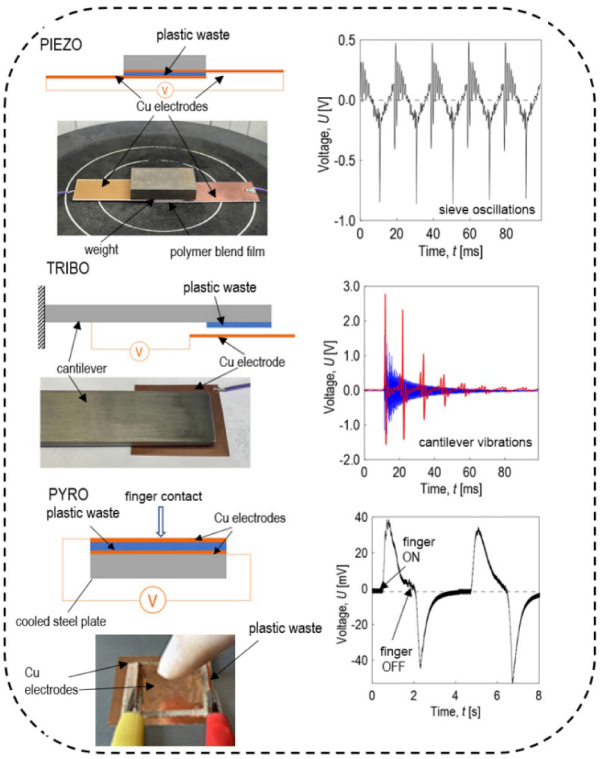

Figure 9. Demonstration of self-powered sensors with a functional layer of polymer film made of unsorted plastic waste (blend B+PET).

cantilever end, and thus adhered tightly to the cantilever after cooling. The collecting Cu electrode (40 × 40 mm) was placed under the cantilever at a distance of 0.35 mm (in red in Figure 9) and 0.05 mm (blue color). The vibrations were caused by the pressure on the beam and its subsequent release.

The practical use of energy induced by the pyroelectric effect from plastic waste was demonstrated using a sensor that detects the heat flow from the finger touch. The sensor was assembled from two copper foil electrodes (30 × 30 mm, thickness 35 μm) with a waste packaging film (thickness 130 μm) between them. The pyroelectric sensor was placed on a steel plate cooled to −18 °C, and heat flow was initiated by applying temperature drop to the sensor (Figure 9 PYRO).

Finally, the possibility of mechanical-electric energy conversion was also demonstrated on the fraction of plastic waste remaining after sorting, which has negligible potential for further usage and is still largely landfilled. This so-called rejected recyclable plastic waste (RRPW) was supplied by recycling company Puruplast a.s., Kostelany nad Moravou, Czech Republic in a form of grind (Figure 10).

DSC and FTIR analyses revealed 90% of polyethylene (PE) originally in the form of packaging films, multilayer PE films, nonwoven fabrics, PE foams, etc., with an HDPE/LDPE ratio of 0.85. The grind also contained PS (mainly beads of expanded PS), PP from films, paper, and dust in unit quantities. Finally, traces of poly(vinylidene chloride), ethylene vinyl acetate copolymer, and PET were detected. RRPW was homogenized in the molten state using a twin-screw mixer (MicroHunter Xplore MC15) at 260 °C for 5 min at 100 rpm. The blend was then compression-molded into 0.25 mm thick (black) films (see Figure 10) for testing. The surface of the RRPW polymer film was relatively fine with Sa = 1.456 μm, Sq = 1.777 μm, and Sz = 10.716 μm. In this way, nanogenerators

https://doi.org/10.1021/acssuschemeng.4c06984
ACS Sustainable Chem. Eng. 2025, 13, 2683−2693

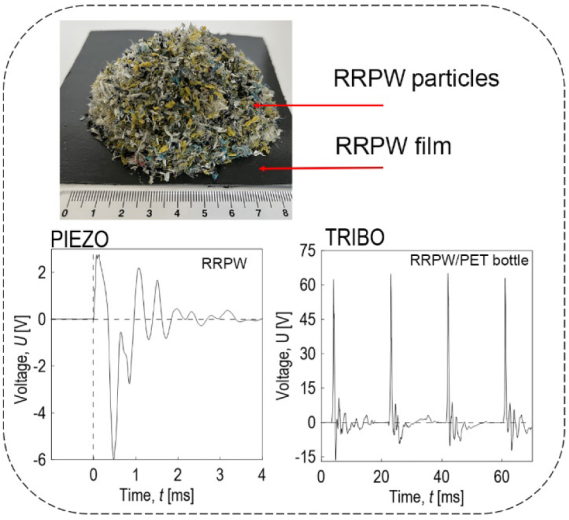

Figure 10. Electrification of rejected recyclable plastic waste (RRPW).

can be fabricated quickly (5 min) without the need for high-tech treatment and equipment.

First, the electrification of the RRPW was tested based on its response to the mechanical compressive stress generated by a pendulum, as schematically shown in Figure 1 PIEZO. During one pendulum impact, the tested sample was compressed to induce an initial voltage (in units of volts). The subsequent fading elastic vibrations of the RRPW film resulted in voltage vibrations that disappeared within four milliseconds. In the TENG built according to Figure 1 TRIBO, the film made from the PET bottle was attached to the anode electrode of the nanogenerator and the RRPW was tribo-positive when paired with a PET bottle. As can be seen from Figure 10, the TENG gave a promising output voltage exceeding 60 V, which is rather higher than that reported for a mixed plastic of PE and PP in a triboelectric pair with polyurethane waste in ref. 23.

DISCUSSION

This study presents unsorted plastic packaging waste as a source of electricity when subjected to external forces and temperature gradients. The obtained output voltages were higher than those previously reported for various plastic wastes (Table 1). The results show that the electric efficiency is enhanced for the mixed plastics compared with the individual ones. Although, the immiscibility of commodity plastics is one of the main issues complicating their recycling and reuse due to unacceptable mechanical performance, it seems to be a key advantage for their electrification.

The key results of this study were obtained as voltage outputs from a triboelectric nanogenerator. Various electrification processes can be combined for the same type of mechanical energy conversion with an integrated electric energy output (coupled electrification) as shown recently for biaxially oriented PET.[25] The nanogenerator (built according to Figure 1 TRIBO) dominantly measures the triboelectric response of waste plastics; however, the piezoelectric and flexoelectric contributions cannot be excluded, as well. Similarly, the tribological effect cannot be omitted during harvesting from pressure pulses after pendulum impact, which results in voltage generation in the individual plastics, their mixture and blends. After one impact of the pendulum, the plastics were compressed, which induced an initial voltage of approximately 4 V for all the plastics tested, except for PS, where the initial voltage was approximately 14 V. It should be stressed that the surface effects and strain gradients can induce flexoelectricity in semicrystalline polymers. The inorganic fillers, which are added to all packaging plastics as processing aids during manufacturing, are piezoelectric (SiO_2) or flexoelectric (TiO_2, $CaCO_3$,), and might contribute to the obtained output voltages as well.

Not even the triboelectrification phenomenon is fully understood.[28] According to Ao et al.[29] steady-state charge is determined by a combination of charge generation (electron transfer,[30] ion transfer,[31] and material transfer[32] and charge dissipation (dielectric breakdown,[33] thermionic emission,[34] and conduction.[35]

In the nanogenerators presented, triboelectric electrification and piezoelectric/flexoelectric electrification occurred simultaneously. The TENG of the PET/PS pair generated an output voltage of over 50 V, which is sufficient to supply self-powered sensors and wearable devices. A peak output voltage of approximately 130 V in one cycle was achieved by using the PET/B+PET triboelectric pair. The pyroelectric response of the individual plastic wastes HDPE, PP, and PS with output voltages around 140 mV is higher than the combinations with PET (which shows the lowest pyroelectric response).

For all of the tested materials, the triboelectric charge density (TECD) was measured to assess the amount of charge generated on the surface during contact. A copper electrode was used as the reference material, providing a baseline for measuring a triboelectric charge density. The triboelectric series of the tested materials are presented in Figure 11. All

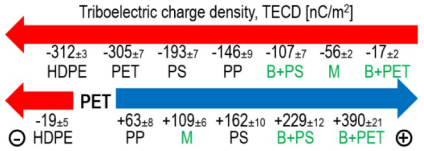

Figure 11. Triboelectric series of individual plastic wastes, their mixture (M) and blends (B+PET and B+PS) relative to copper (top) and PET (bottom).

tested materials are electronegative relative to copper, meaning that they acquire a negative charge when in contact with copper. The tribo-negative character of the individual plastic wastes increases as follows: PP, PS, PET, and HDPE. Their mixture (M) and blends (B+PE and B+PS) exhibited a lower TECD than the individual waste components; the lowest TECD value was obtained for the B+PET blend. This antagonistic effect, where a compound shows lower properties than its individual components, highlights the importance of complex interactions within the compounds, leading to a reduced tribo-negative character. This relationship is a fundamental finding that significantly influences the electrification parameters, when combining materials into an experimental TENG. We believe that this phenomenon is largely induced by the general immiscibility of the polymers and formation of immiscible polymer blends and mixtures.

As shown throughout the paper, a PET bottle was chosen as the second counter electrode for the tested materials in the TENG construction. It is tribo-negative to all tested materials except HDPE, with a TECD value of 305 nC/m^2 relative to the reference copper electrode, as shown in Figure 11 (bottom). The most efficient TENG, in terms of material

https://doi.org/10.1021/acssuschemeng.4c06984
ACS Sustainable Chem. Eng. 2025, 13, 2683−2693

composition, is the tribological pair of PET and B+PET. The TECD value for PET and the B+PET blend was 390 nC/m^2.

The obtained results support the idea that the primary and most significant factor influencing the generation of triboelectric energy is the selection of materials for the triboelectric positive and negative layers. The triboelectric positive layer composed of 60% recycled PET with an equal distribution of PS, HDPE, and PP (referred to as B+PET blend) is less negative than the layers made from other mixtures, as shown in Figure 11. Additionally, the tribo-positive layer of B+PET exhibited a lower relative permittivity compared with the same layer made from other blends. The combination of these properties has a fundamental effect on triboelectric energy generation.

We focused on primary factors, such as triboelectric properties and relative permittivity, which can be reliably controlled through the composition of the mixture. This approach ensured sufficient reproducibility of the results. Nevertheless, a significant direction for further improvement in the performance of triboelectric devices lies in the optimization of material surface properties,[36] where key factors include surface roughness, adhesion,[37] and presence of fillers (nanoparticles). It has been found[38] that the surface roughness of polymers such as LDPE, HDPE, and PS directly affects the generation of surface charge; coarser surfaces led to higher surface charges, enhancing the efficiency of nanogenerators. Monitoring the polarity of the charge during contact showed that smoother polymer surfaces always generate negative charges during contact electrification.[39] Furthermore, contact electrification can be controlled by intramolecular forces in the polymer bulk and adhesive forces at the contact interface.[40] The findings suggest that controlling the surface roughness and type of adhesion could open new possibilities for improving the performance of triboelectric devices and sensors.

Surface viscoelasticity has been identified as another key parameter for improving triboelectric performance.[41,42] Mechanical properties might enhance the synergic effect of plastic waste compounds (mixtures and blends) in comparison to that of individual wastes. Different moduli of the noncompatible plastic waste compounds (see Supporting Information) result in heterogeneous hardness, which may support the creation of regions of increased stress concentration, promoting mechanisms of contact triboelectrification, which enhance the output of triboelectric charge.

All principles of electrification, such as piezo-, tribo-, and pyro-electrification, can be advantageously used for the construction of self-powered sensors of external stimuli. Examples of sensing systems present solutions sensitive enough to detect the stimulus in real time repeatedly and durably. As a functional element of the sensor, it is sufficient to use a polymer film equipped with suitable collection electrodes. In comparison to the robust TENG (e.g., in,[43] this solution is rather simple from the point of view of polymer processing technology; a functional sensor from plastic waste can be prepared in-house as well. The films are flexible, relatively soft, and can be simply fixed in the molten state on, e.g., iron parts; thus, their design can be easily modified and tailored for an application.

Finally, the output voltage stability over 1000 cycles was tested using a B+PET blend and PET bottle tribological pairs to demonstrate the reliability of the mixed plastic wastes under repeated mechanical loading. A schematic of the arrangement of the electrodes and polymer films is depicted in Figure 12. The results demonstrated consistent and stable outputs with voltage levels of approximately 58 V.

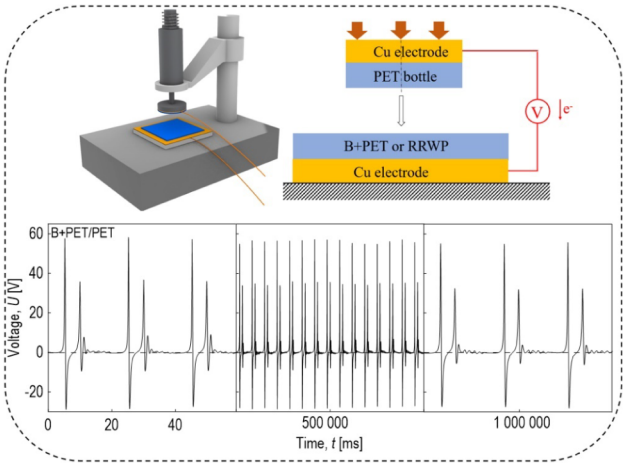

Figure 12. Schematic arrangement of the triboelectric contact-separation setup and output voltages for B+PET during 1000 cycles.

CONCLUSION

In this study, the possibility of using mixed and unsorted postconsumer plastic waste for the generation of electric energy through triboelectricity, piezoelectricity, and pyroelectricity was presented. Individual plastics and their mixtures and blends were analyzed with a focus on the conversion of mechanical energy and the imposed temperature gradient to electricity. Considering the challenges associated with recycling these materials due to their immiscibility, the high output voltage achieved with mixed plastic waste, which surpasses previous reports for various plastic waste types, is a notable advantage of the proposed nanogenerators. Interestingly, immiscibility, which is typically an obstacle in the recycling process, appears to be beneficial for electrification.

Triboelectric charge density (TECD) measurements show that mixtures and blends of plastic wastes exhibit a lower TECD than individual plastics. This antagonistic effect highlights the importance of carefully selecting the composition of plastic waste for optimal energy harvesting. There are several further challenges and drawbacks to consider, as the understanding of the electrification phenomenon remains incomplete, particularly concerning the role of surface effects, strain gradients, and complex interactions between the materials, which can affect the consistency of the generated voltages. Additionally, the use of inorganic fillers such as SiO_2, TiO_2, and $CaCO_3$ may contribute to voltage generation but could also introduce variability in the results because of their complex interactions with the polymer matrices.

Furthermore, the interpolymer triboelectric interactions influence the output voltage in a favorable direction also for the so-called rejected recyclable plastic waste (RRPW), which as a part of waste in containers remaining after sorting, and is, in the vast majority, landfilled. TENG prepared from RRPW with simple and inexpensive melt mixing and compression molding showed promising output voltage responses. Therefore, harvesting electricity from unseparated postconsumer waste, including RRPW with almost zero potential for other uses, may supplement electric energy sources.

https://doi.org/10.1021/acssuschemeng.4c06984
ACS Sustainable Chem. Eng. 2025, 13, 2683−2693

This is a promising result that increases the possibility of reusing unsorted consumer waste materials, including rejected recyclable plastic waste, without any demanding and often environmentally tasking treatment techniques and the incorporation of potentially hazardous materials. The challenges related to material compatibility and complex interactions between components must be addressed to fully realize the potential of these nanogenerators in robust applications.

■ ASSOCIATED CONTENT

Data Availability Statement

The data are available at 10.5281/zenodo.13347648.

Supporting Information

The Supporting Information is available free of charge at https://pubs.acs.org/doi/10.1021/acssuschemeng.4c06984.

Mechanical properties in terms of Young modulus, tensile strength and ductility of the individual waste plastics (HDPE, PP, PS, PET), mixture M, blend B +PET, and blend B+PS (PDF)

■ AUTHOR INFORMATION

Corresponding Author

Berenika Hausnerova − *Centre of Polymer Systems, University Institute Tomas Bata University, Zlin 76001, Czech Republic; Department of Production Engineering, Tomas Bata University in Zlin:Faculty of Technology, Zlin 760 01, Czech Republic;* orcid.org/0000-0002-6368-7896; Email: hausnerova@utb.cz

Authors

Petr Slobodian − *Centre of Polymer Systems, University Institute Tomas Bata University, Zlin 76001, Czech Republic; Department of Physics and Materials Engineering, Tomas Bata University in Zlín:Faculty of Technology, Zlín 760 01, Czech Republic*

Pavel Riha − *Department of Physics and Materials Engineering, Tomas Bata University in Zlín:Faculty of Technology, Zlín 760 01, Czech Republic; Department of Production Engineering, Tomas Bata University in Zlin:Faculty of Technology, Zlin 760 01, Czech Republic*

Complete contact information is available at: https://pubs.acs.org/10.1021/acssuschemeng.4c06984

Notes

The authors declare no competing financial interest.

■ ACKNOWLEDGMENTS

This work was also supported by the Ministry of Education, Youth, and Sports of the Czech Republic (DKRVO, RP/CPS/2024-28). Vladimir Pata is acknowledged for the evaluation of the surface parameters.

■ REFERENCES

(1) *Global plastics industry - statistics & facts*, https://www.statista.com/topics/5266/plastics-industry/; accessed on July, 2024.

(2) Hernández, B.; Vlachos, D. G.; Ierapetritou, M. G. Superstructure optimization for management of low-density polyethylene plastic waste. *Green Chem.* **2024**, *26*, 9476.

(3) Kalali, E. N.; Lotfian, S.; Shabestari, M. E.; Khayatzadeh, S.; Zhao, C.; Nezhad, H. Y. A critical review of the current progress of plastic waste recycling technology in structural materials. *Curr. Opin. Green Sustainable Chem.* **2023**, *40*, 100763.

(4) Ligero, A.; Solís, R. R.; Blázquez, G.; Munoz-Batista, M. J.; Pérez, A.; Calero, M. On the cutting-edge of non-recyclable plastic waste valorization: From pyrolysis char to nitrogen-enriched activated carbon for landfill biogas upgrading. *J. Environ. Chem. Eng.* **2024**, *12*, 112265.

(5) Mahrous, R.; Giancola, E.; Osman, A.; Asawa, T.; Mahmoud, H. Alternative to PCM: Recycling Plastic Waste for Affordable Thermal Insulation in Building Envelopes: An Experimental Analysis. *Future Cities Environ.* **2024**, *10* (1), 1−15.

(6) Wang, H.; Ng, L. S.; Li, H.; Lee, H. K.; Han, J. Achieving milliwatt level solar-to-pyroelectric energy harvesting via simultaneous boost to photothermal conversion and thermal diffusivity. *Nano Energy* **2023**, *108*, 108184.

(7) Wang, K.; Liu, Q.; Zhang, Q.; Xiang, Y.; Hu, X. Display integrated flexible and transparent large-area pyroelectric gesture recognition/piezoelectric touch control sensor array based on in-situ polarized PVDF-TrFE films. *Sens Actuators A Phys.* **2023**, *357*, 114406.

(8) Amangeldinova, Y.; Oh, J.- W.; Lee, W.; Shin, D.- M.; Hwang, Y.- H. A Study of Contact Electrification Process on PVDF−Metal Interface: Effect of β Phase Composition. *Adv. Mater. Interface* **2024**, *11* (6), 2300727.

(9) Ong, D. T. K.; Koay, J. S. C.; Sim, M. T.; Aw, K. C.; Nakajima, T.; Chen, B.; Tan, S. T.; Gan, W. C. High performance composition-tailored PVDF triboelectric nanogenerator enabled by low temperature-induced phase transition. *Nano Energy* **2023**, *113*, 108555.

(10) Shafeek, S.; Balakrishnan, N. T. M.; Fatma, B.; Garg, A.; Fatima, J. M. J.; Morton, D.; Luo, J.; Raghavan, P. Exalting energy scavenging for triboelectric nanogenerator using silicon carbide particles doped polyvinylidene difluoride nanocomposite. *Nano Energy* **2023**, *107*, 108146.

(11) Gupta, S.; Chatterjee, C.; Fatma, B.; Brajesh, K.; Bhunia, R.; Sowmya, N. S.; Roy, S.; Kulkarni, A.; Gupta, R. K.; Gupta, R.; Ajayan, P. M.; Garg, A. Functionality Tuning in Hierarchically Engineered Magnetoelectric Nanocomposites for Energy-Harvesting Applications. *ACS Appl. Mater. Interfaces* **2023**, *15*, 26563−26575.

(12) Han, G.; Wu, B.; Pu, Y. A triboelectric nanogenerator based on waste plastic bags for flexible vertical interconnection system. *Microsyst. Technol.* **2020**, *26*, 3893−3899.

(13) Rani, G. M.; Wu, C. M.; Motora, K. G.; Umapathi, R. Waste-to-energy: Utilization of recycled waste materials to fabricate triboelectric nanogenerator for mechanical energy harvesting. *J. Cleaner Prod.* **2022**, *363*, 132532.

(14) Nawaz, S. M.; Saha, M.; Sepay, N.; Mallik, A. Energy-from-waste: A triboelectric nanogenerator fabricated from waste polystyrene for energy harvesting and self-powered sensor. *Nano Energy* **2022**, *104*, 107902.

(15) Sherrell, P. C.; Šutka, A.; Timusk, M.; Šutka, A. Alternatives to Fluoropolymers for Motion-Based Energy Harvesting: Perspectives on Piezoelectricity, Triboelectricity, Ferroelectrets, and Flexoelectricity. *Small* **2024**, *20* (32), 2311570.

(16) Šutka, A.; Šutka, A.; Dundurs, H.; Del Rosal, B.; Iesalnieks, M.; Malnieks, K.; Linarts, A.; Barlow, A. J.; Leon, R. T.; Ellis, A. V.; Sherrell, P. C. Recycled Polystyrene Waste to Triboelectric Nanogenerators: Volumetric Electromechanically Responsive Laminates from Same-Material Contact Electrification. *Adv. Energy Sust. Res.* **2024**, *5* (6), 2300259.

(17) Bukhari, M. U.; Khan, A.; Maqbool, K. Q.; Arshad, A.; Riaz, K.; Bermak, A. Waste to Energy: Facile, Low-Cost and Environment-Friendly Triboelectric Nanogenerators Using Recycled Plastic and Electronic Wastes for Self-Powered Portable Electronics. *Energy Rep.* **2022**, *8*, 1687−1695.

(18) Feng, X.; Li, Q.; Wang, K. Waste Plastic Triboelectric Nanogenerators Using Recycled Plastic Bags for Power Generation. *ACS Appl. Mater. Interfaces* **2021**, *13* (1), 400−410.

(19) Das, N. K.; Badhulika, S. Recyclable waste derived green triboelectric nanogenerator for Self-Powered synthesis of Defect-Free

graphene via Mechano-Electrochemical exfoliation. *Chem. Eng. J.* **2024**, *480*, 147897.
(20) Navaneeth, M.; Potu, S.; Babu, A.; Lakshakoti, B.; Rajaboina, R. K.; Kumar, U. K.; Divi, H.; Kodali, P.; Balaji, K. Transforming Medical Plastic Waste into High-Performance Triboelectric Nanogenerators for Sustainable Energy, Health Monitoring, and Sensing Applications. *ACS Sust. Chem. Eng.* **2023**, *11* (32), 12145−12154.
(21) Varghese, H.; Chandran, A. Triboelectric nanogenerator from used surgical face mask and waste mylar materials aiding the circular economy. *ACS Appl. Mater. Interfaces* **2021**, *13*, 51132−51140.
(22) Sahu, M.; Hajra, S.; Kim, H. G.; Rubahn, H. G.; Kumar Mishra, Y.; Kim, H. J. Additive manufacturing-based recycling of laboratory waste into energy harvesting device for self-powered applications. *Nano Energy* **2021**, *88*, 106255.
(23) Khandelwal, G.; Chandrasekhar, A.; Alluri, N. R.; Vivekananthan, V.; Raj, N. P. M. J.; Kim, S.-J. Trash to Energy: A Facile, Robust and Cheap Approach for Mitigating Environment Pollutant Using Household Triboelectric Nanogenerator. *Appl. Energy* **2018**, *219*, 338−349.
(24) Stepancikova, R.; Olejnik, R.; Matyas, J.; Masar, M.; Hausnerova, B.; Slobodian, P. Pressure-Driven Piezoelectric Sensors and Energy Harvesting in Biaxially Oriented Polyethylene Terephthalate Film. *Sensors* **2024**, *24*, 1275.
(25) Slobodian, P.; Olejnik, R.; Matyas, J.; Riha, P.; Hausnerova, B. A coupled piezo-triboelectric nanogenerator based on the electrification of biaxially oriented polyethylene terephthalate food packaging films. *Nano Energy* **2023**, *118*, 108986.
(26) Pan, D.; Su, F.; Liu, C.; Guo, Z. Research progress for plastic waste management and manufacture of value-added products. *Adv. Compos. Hybrd. Mater.* **2020**, *3*, 443−461.
(27) Padha, B.; Verma, S.; Prerna; Ahmed, A.; Patole, S. P.; Arya, S. Plastic turned into MXene−based pyro-piezoelectric hybrid nanogenerator-driven self-powered wearable symmetric supercapacitor. *Appl. Energy* **2024**, *356*, 122402.
(28) Shin, E. C.; Ko, J. H.; Lyeo, H. K.; Kim, Y. H. Derivation of a governing rule in triboelectric charging and series from thermoelectricity. *Phys. Rev. Res.* **2022**, *4*, 023131.
(29) Ao, C. K.; Jiang, Y.; Zhang, L.; Yan, C.; Ma, J.; Liu, C.; Jiang, Y.; Zhang, W.; Soh, S. Balancing charge dissipation and generation: mechanisms and strategies for achieving steady-state charge of contact electrification at interfaces of matter. *J. Mater. Chem. A* **2022**, *10*, 19572−19605.
(30) Gallo, C. F.; Lama, W. L. Some charge exchange phenomena explained by a classical model of the work function. *J. Electrost.* **1976**, *2*, 145−150.
(31) McCarty, L. S.; Winkleman, A.; Whitesides, G. M. Ionic electrets: electrostatic charging of surfaces by transferring mobile ions upon contact. *J. Am. Chem. Soc.* **2007**, *129*, 4075−4088.
(32) Baytekin, H. T.; Patashinski, A. Z.; Branicki, M.; Baytekin, B.; Soh, S.; Grzybowski, B. A. The mosaic of surface charge in contact electrification. *Science* **2011**, *333* (6040), 308−312.
(33) Liu, D.; Zhou, L.; Li, S.; Zhao, Z.; Yin, X.; Yi, Z.; Zhang, C.; Li, X.; Wang, J.; Wang, Z. L. Hugely enhanced output power of direct-current triboelectric nanogenerators by using electrostatic breakdown effect. *Adv. Mater. Technol.* **2020**, *5* (7), 2000289.
(34) Xu, C.; Zi, Y.; Wang, A. C.; Zou, H.; Dai, Y.; He, X.; Wang, P.; Wang, Y.-C.; Feng, P.; Li, D.; Wang, Z. L. On the electron-transfer mechanism in the contact-electrification effect. *Adv. Mater.* **2018**, *30* (15), 1706790.
(35) Kinders Berger, J.; Lederle, C. Surface charge decay on insulators in air and sulfur hexafluorid-part II: measurements. *IEEE Trans. Dielectr. Electr. Insul.* **2008**, *15*, 949−957.
(36) Šutka, A.; Malnieks, K.; Lapčinskis, L.; Timusk, M.; Kalnins, K.; Kovalovs, A.; Bitenieks, J.; Knite, M.; Stevens, D.; Grunlan, J. Contact electrification between identical polymers as the basis for triboelectric/flexoelectric materials. *Phys. Chem. Chem. Phys.* **2020**, *22*, 13299−13305.
(37) Lapčinskis, L.; Malnieks, K.; Blums, J.; Knite, M.; Oras, S.; Käämbre, T.; Vlassov, S.; Antsov, M.; Timusk, M.; Šutka, A. The adhesion-enhanced contact electrification and efficiency of triboelectric nanogenerators. *Macromol. Mater. Eng.* **2020**, *305* (1), 1900638.
(38) Sherrell, P. C.; Šutka, A.; Shepelin, N. A.; Lapcinskis, L.; Verners, O.; Germane, L.; Timusk, M.; Fenati, R. A.; Malnieks, K.; Ellis, A. V. Probing contact electrification: a cohesively sticky problem. *ACS Appl. Mater. Interfaces* **2021**, *13* (37), 44935−44947.
(39) Verners, O.; Lapčinskis, L.; Germane, L.; Kasikov, A.; Timusk, M.; Pudzs, K.; Ellis, A. V.; Sherrell, P. C.; Šutka, A. Smooth polymers charge negatively: Controlling contact electrification polarity in polymers. *Nano Energy* **2022**, *104*, 107914.
(40) Šutka, A.; Malnieks, K.; Lapčinskis, L.; Kaufelde, P.; Linarts, A.; Berziņa, A.; Zables, R.; Jurkans, V.; Gornevs, I.; Blums, J.; Knite, M. The role of intermolecular forces in contact electrification on polymer surfaces and triboelectric nanogenerators. *Energy Environ. Sci.* **2019**, *12* (8), 2417−2421.
(41) Lapčinskis, L.; Linarts, A.; Malnieks, K.; Kim, H.; Rubenis, K.; Pudzs, K.; Smits, K.; Kovalovs, A.; Klanins, K.; Tamm, A.; Jeong, C. K.; Šutka, A. Triboelectrification of nanocomposites using identical polymer matrixes with different concentrations of nanoparticle fillers. *J. Mater. Chem. A* **2021**, *9* (14), 8984−8990.
(42) Šutka, A.; Lapčinskis, L.; Verners, O.; Germane, L.; Smits, K.; Pludons, A.; Gaidukovs, S.; Jerane, I.; Zubkins, M.; Pudzs, K.; Sherrell, P. C.; Blums, J. Bio-Inspired Macromolecular Ordering of Elastomers for Enhanced Contact Electrification and Triboelectric Energy Harvesting. *Adv. Mater. Technol.* **2022**, *7* (10), 2200162.
(43) Fatma, B.; Gupta, S.; Chatterjee, C.; Bhunia, R.; Verma, V.; Garg, A. Triboelectric generators made of mechanically robust PVDF films as self-powered autonomous sensors for wireless transmission based remote security systems. *J. Mater. Chem. A* **2020**, *8*, 15023−15033.

https://doi.org/10.1021/acssuschemeng.4c06984
ACS Sustainable Chem. Eng. 2025, 13, 2683−2693